

1 **Spatio-Temporal Models of Intermediate Complexity for Ecosystem**

2 **Assessments: a new tool for spatial fisheries management**

3
4 James T. Thorson^{1*}, Grant Adams², Kirstin Holsman³

5
6 ¹ Habitat and Ecosystem Process Research program, Alaska Fisheries Science Center, NMFS,
7 NOAA, Seattle, WA, USA

8 ² School of Aquatic and Fisheries Sciences, University of Washington, Seattle, WA, USA

9 ³ Resource Ecology and Fisheries Management program, Alaska Fisheries Science Center,
10 NMFS, NOAA, Seattle, WA, USA

11
12 * Corresponding author

13 James.Thorson@noaa.gov

14
15 Running header: MICE-in-space models

16

17

18

19

20 **Abstract**

21 Multispecies models are widely used to evaluate management trade-offs arising from species
22 interactions. However, identifying climate impacts and sensitive habitats requires integrating
23 spatial heterogeneity and environmental impacts into multispecies models at fine spatial scales.
24 We therefore develop a spatio-temporal model of intermediate complexity for ecosystem
25 assessments (a “MICE-in-space”), which is fitted to survey sampling data and time-series of
26 fishing mortality using maximum likelihood techniques. The model is implemented in the *VAST*
27 R package, and it can be configured to range from purely descriptive to including ratio-
28 dependent interactions among species. We demonstrate this model using data for four
29 groundfishes in the Gulf of Alaska using data from 1982-2015. Model selection for this case
30 study shows that models with species interactions are parsimonious, although a model specifying
31 separate density dependence without interactions also has substantial support. The AIC-selected
32 model estimates a significant, negative impact of Alaska pollock (*Gadus chalcogrammus*,
33 Gadidae) on productivity of other species and suggests that recent fishing mortality for Pacific
34 cod (*G. microcephalus*, Gadidae) is above the biological reference point (BRP) resulting in 40%
35 of unfished biomass; other models show similar trends but different scales due to different BRP
36 estimates. A simulation experiment shows that fitting a model with fewer species at a coarse
37 spatial resolution degrades estimation performance, but that interactions and biological reference
38 points can still be estimated accurately. We conclude that MICE-in-space models can
39 simultaneously estimate fishing impacts, species-tradeoffs, biological reference points, and
40 habitat quality. They are therefore suitable to forecast short-term climate impacts, optimize
41 survey designs, and designate protected habitats.

42

43 Keywords: ecosystem model; models of intermediate complexity for ecosystem assessments;

44 essential fish habitat; spatio-temporal model; VAST

45

46 **Table of contents:**

47 1. Introduction

48 2. Methods

49 a. Index-standardization model as starting point

50 b. Extending the model to account for species interactions

51 c. Parameter estimation

52 d. Case study application

53 e. Simulation experiment

54 3. Results

55 4. Discussion

56 a. Projecting climate impacts

57 b. Optimizing survey designs

58 c. Designation of essential fish habitat

59 d. Multi-model inference regarding status and productivity

60 e. Future research

61 5. Acknowledgements

62

63 **1. Introduction**

64 Fisheries managers use a mix of different management instruments to regulate fishing and
65 other marine impacts (Walther and Möllmann 2014; Dolan *et al.* 2016). Scientific advice to
66 support fisheries management typically includes (but is not limited to): limits on fishery landings
67 and incidental catch for individual species; spatial regulation of activities occurring near
68 sensitive habitats or species; ecosystem-based limits on total landings and fishing gears; and
69 allocation of species quotas to different ports or fleets based on forecasted changes in species
70 distribution or productivity. These four examples are informed, respectively, by analysis of
71 stock status, habitat quality, ecosystem function, and climate linkages, and fisheries science is
72 developing tools to implement these four types of analysis rapidly, transparently, and at low cost.
73 Fisheries managers have benefited from tools that can be used for multiple types of analysis, e.g.,
74 by using “models of intermediate complexity for ecosystem assessments” (MICE; Plagányi *et al.*
75 2014) to simultaneously analyze stock status and multispecies tradeoffs.

76 The dynamics of marine species is regulated by biological interactions such as predation and
77 competition, and also impacted by technical interactions arising from shared impacts of fishing
78 activities (Gaichas *et al.* 2010; Pikitch *et al.* 2014; Spencer *et al.* 2016). As a result, harvesting
79 can impact target species directly, and also impact interdependent species indirectly through
80 changes in natural mortality and resource availability (Reum *et al.* 2019; Collie and Gislason
81 2001). The indirect impact of harvesting on non-target species may be counterintuitive, and
82 fisheries management requires information regarding these impacts both to mitigate fishing
83 impacts on unproductive species as well as to identify management strategies that are expected to
84 perform well for a variety of stakeholders (Plagányi *et al.* 2011; Marshall *et al.* 2019).

85 Fisheries managers therefore use ecosystem models to identify potential trade-offs of
86 management decisions that arise from biological and technical interactions (Hollowed 2000;
87 Lassen *et al.* 2013; Plagányi *et al.* 2014). Ecosystem models can vary in complexity from
88 models of intermediate complexity for ecosystem assessments (MICE), which estimate
89 population parameters for a subset of key interacting species from time-series of data, to end-to-
90 end whole ecosystem models that simulate the interactions of multiple oceanographic,
91 ecological, and anthropogenic processes (Plagányi *et al.* 2011; Collie *et al.* 2016; Ortiz *et al.*
92 2016). However, a key aspect of ecosystem models is that they incorporate processes such as
93 predation, competition, and fishing (Plagányi and Butterworth 2012; Ortiz *et al.* 2016;
94 Mackinson *et al.* 2018). These models are typically used to forecast changes in population
95 density, productivity, and fishery catch under alternative management procedures and
96 environmental conditions, and forecasts will likely be improved via explicit inclusion of
97 biological and technical interactions (Howell and Filin 2014; Tommasi *et al.* 2017).

98 Global climate change is causing rapid shifts in the spatial distribution of physical habitat,
99 nutrients, forage species, and predators. These shifts can cause rapid changes in structure and
100 productivity for the ecosystem managed by a given jurisdiction. Models that fail to account for
101 ecosystem changes resulting from spatial shifts are less likely to accurately forecast performance
102 of alternative management procedures, and in some cases will have degraded performance when
103 informing fisheries management (Kempf *et al.* 2010; Spencer *et al.* 2016; Fu *et al.* 2017). One
104 avenue to account for ecosystem changes resulting from spatial distribution shifts is to develop
105 ecosystem models that estimate variation in species density and/or productivity at fine-spatial
106 scales while also accounting for species interactions (see review in Hunsicker *et al.* 2011)

107 Spatially-explicit ecosystem models are currently used to inform spatial planning, identify
108 tradeoffs for alternative management strategies, and provide annual advice regarding limits on
109 fishery harvest. Spatially-explicit ecosystem models that are widely used include Atlantis
110 (Fulton *et al.* 2011), OSMOSE (Shin and Cury 2001), EwE (Christensen and Walters 2004), and
111 Gadget (Begley and Howell 2004), and these existing models vary in the extent to which users
112 must “tune them by hand” prior to further model usage. Ideally, spatially-explicit ecosystem
113 models would have good statistical properties (e.g., statistical consistency and well-defined
114 forecast intervals; (Magnusson *et al.* 2013)), would assimilate available data (e.g., resource
115 surveys) through probabilistic estimation methods, and could provide biological reference points
116 for harvest recommendations. In parallel, there is a growing literature developing multispecies
117 spatio-temporal models to predict variation in density at fine spatial scales while estimating
118 spatial correlation functions that are used to interpolate and extrapolate population density to
119 unsampled locations (Ovaskainen *et al.* 2017; Thorson *et al.* 2017; Schliep *et al.* 2018).
120 However, these previous approaches have not explicitly included fishing mortality, and therefore
121 have not been capable of estimating biological reference points for regulating fishery catches.

122 We therefore develop a spatio-temporal multispecies model including species interactions,
123 fishing mortality, and estimating fishing mortality and biomass relative to biological reference
124 points that are commonly used in stock assessment. This spatio-temporal model has structural
125 complexity intermediate between single-species and end-to-end ecosystem models while
126 accounting for spatial variation, so we call it a “Spatial model of intermediate complexity for
127 Ecosystem assessments” (MICE-in-space). It fits directly to survey data using maximum-
128 likelihood techniques, and assumes that biological interactions depend upon local densities of
129 modeled species. To do so, we extend an existing vector-autoregressive spatio-temporal

130 modelling framework, implemented using package *VAST* (Thorson and Barnett 2017), which has
131 been used previously for stock assessments, ecosystem status reports, and journal articles in
132 many regions worldwide (see Thorson (2019b) for examples). We then demonstrate this MICE-
133 in-space model by application to survey data for four species in the Gulf of Alaska, and use a
134 simulation experiment conditioned on this case study to explore the statistical properties of the
135 model. Through development of generic software, we envision that MICE-in-space models will
136 help further align stock, ecosystem, and habitat assessments, and improve future ecosystem-
137 based management advice.

138 **2. Methods**

139 We seek to develop an approach that combines features of three existing types of models
140 used in marine ecosystems:

- 141 1. Spatially explicit models can be broadly categorized as “spatially stratified” or “spatio-
142 temporal” models (Berger *et al.* 2017). Spatially stratified models have a long history in
143 population and ecosystem modelling (Beverton and Holt 1957; Goethel *et al.* 2011), but
144 typically cannot be fitted to data representing dynamics occurring at fine spatial scales
145 because the amount of data per stratum decreases as the number of spatial strata is increased.
146 By contrast, we develop a spatio-temporal model that incorporates a spatial correlation
147 function to approximate dynamics occurring continuously across space (Cressie and Wikle
148 2011; Kristensen *et al.* 2014), such that the spatial resolution of the model can be
149 manipulated with relatively small changes in model performance. Although there have been
150 previous “spatio-temporal multispecies models” (e.g., Walters and Bonfil 1999), they
151 typically have not been fitted statistically using techniques that estimate uncertainty.

152 2. Models of Intermediate Complexity (MICE), which represent dynamics for 2-10 species;
153 explicitly consider environmental, ecological, anthropogenic, and management trade-offs;
154 and fit to available data in a probabilistic framework that allows for model validation similar
155 to conventional single-species models (Plagányi 2007). Specifically, our MICE-in-space
156 model can fit a similar number of species while estimating parameters and generating
157 probabilistic forecasts of spatio-temporal dynamics.

158 3. Joint dynamic species distribution models (JDSDM), which estimate population density
159 including the degree of spatial autocorrelation; account for covariation in density and
160 productivity among multiple species; and incorporate changes in spatial distribution for
161 multiple species over time (Thorson *et al.* 2016). Specifically, the MICE-in-space model
162 identifies the predicted mix of species encountered at any given location, thereby providing
163 an estimate of likely technical interactions (e.g., Dolder *et al.* 2018).

164 Finally, we seek to combine these elements in a manner that allows ecologists to explore nested
165 changes in model structure that scale in structural complexity from descriptive (i.e., without
166 explicit models for species dynamics and interactions) through stacked single-species models
167 (i.e., independent dynamics for each species) to multi-species models (i.e., explicitly considering
168 species interactions). To accomplish these goals, we develop a model as follows.

169 **2.1 Index-standardization model as starting point**

170 We start by modelling biomass-density $d(s, c, t)$ for each category c (in this case representing
171 different species), location s , and year t while fitting to samples of biomass, where b_i is the i -th
172 sample (of I total samples), and this sample records biomass at location s_i for category c_i and
173 year t_i (of S locations, C categories, and T years total). We first describe the simplest

174 multispecies spatio-temporal model configuration, which we call an “index standardization”
175 model, and then describe how it is modified to approximate species interactions.

176 First, we adapt an existing Poisson-link delta model (Thorson 2018) that specifies the
177 probability $\Pr(b_i = B)$ that the i -th sample b_i would yield a biomass of B . This model specifies
178 this probability using numbers-density $n(s, c, t)$ and biomass-per-individual $w(s, c, t)$, where
179 $d(s, c, t) = n(s, c, t) \times w(s, c, t)$:

$$\Pr(b_i = B) = \begin{cases} 1 - p_i & \text{if } B = 0 \\ p_i \times g(B|r_i, \sigma^2(c)) & \text{if } B > 0 \end{cases} \quad (1)$$

180 where encounter probability $p_i = \exp(-a_i \times n(s_i, c_i, t_i))$ follows a Poisson process given
181 numbers density and the area swept a_i by the i -th sample. Similarly, the expected biomass given
182 that a sample encounters the species, r_i , is defined such expected biomass $\mathbb{E}(B) = p_i \times r_i$, which
183 yields $r_i = a_i \times n(s_i, c_i, t_i) \times w(s_i, c_i, t_i)/p(i)$, such that r_i is affected by both numbers density
184 and biomass-per-individual. Finally, $g(B|r_i, \sigma^2(c_i))$ is a probability density function for
185 unexplained variation in positive catch rates given residual sampling variance $\sigma^2(c_i)$. This
186 Poisson-link delta model is numerically efficient approximation to the compound Poisson-
187 gamma distribution (Foster and Bravington 2013). We use it in the following because we will
188 later approximate species interactions as a linear model for log-density, and the Poisson-link
189 delta model allows us to predict biomass-sampling data while accounting for spatial and
190 temporal variation in log-density.

191 Each component of the index-standardization model then has a separate intercept for each
192 species and year ($\beta_n(c, t)$ and $\beta_w(c, t)$), where these intercepts account for differences in
193 average density among species (e.g., due to different equilibrium densities in the community,
194 corresponding to different $\beta_n(c, t)$ for each species c) and over time (e.g., due to different levels

195 of spatial aggregation, captured via differences in $\beta_w(c, t)$ among years t). Each component also
 196 includes “spatial variation,” which is constant over time ($\omega_n(s, c)$ and $\omega_w(s, c)$), as well as
 197 “spatio-temporal variation,” which varies over time ($\varepsilon_n(s, c, t)$ and $\varepsilon_w(s, c, t)$):

$$\begin{aligned} \log(n(s, c, t)) &= \beta_n(c, t) + \omega_n(s, c) + \varepsilon_n(s, c, t) \\ \log(w(s, c, t)) &= \beta_w(c, t) + \omega_w(s, c) + \varepsilon_w(s, c, t) \end{aligned} \quad (2)$$

198 where spatial variation is estimated while specifying a multivariate probability distribution for
 199 $\omega_n(s, c)$ and $\omega_w(s, c)$:

$$\mathbf{\Omega}_n \sim MVN(\mathbf{0}, \mathbf{R}(\kappa_n, \mathbf{H}) \otimes \mathbf{L}_{\omega_n} \mathbf{L}_{\omega_n}^T) \quad (3)$$

200 where $\mathbf{\Omega}_n$ is the matrix of spatial variation $\omega_n(s, c)$, and $\mathbf{R}(\kappa_n, \mathbf{H})$ is a matrix of spatial
 201 correlations among locations s given estimated decorrelation rate κ_n and a transformation matrix
 202 \mathbf{H} . Estimated matrix \mathbf{H} represents the tendency for spatial correlations to decline faster in some
 203 directions than others, e.g., where ecosystems with a large variation in depth may tend to have to
 204 have spatial correlations that decline faster moving perpendicular to depth gradients than along
 205 those gradients. We model spatial correlations using a stationary Matérn correlation function
 206 although future studies could explore alternative spatial processes, e.g., where correlations vary
 207 as a function of local environmental conditions (e.g., Fuglstad *et al.*, 2015). Meanwhile, \mathbf{L}_{ω_n} is a
 208 triangular matrix representing species associations with one or more estimated “spatial factors,”
 209 such that $\mathbf{L}_{\omega_n} \mathbf{L}_{\omega_n}^T$ is the estimated covariance in spatial distribution (e.g., Pollock *et al.* 2014),
 210 and we define an identical distribution for $\mathbf{\Omega}_w$, except involving a separate estimate of κ_w and
 211 \mathbf{L}_{ω_w} .

212 The index-standardization model specifies that spatio-temporal variation is independent in
 213 each year:

$$vec(\mathbf{E}_n(t)) \sim MVN(\mathbf{0}, \mathbf{R}(\kappa_n) \otimes \mathbf{L}_{\varepsilon n} \mathbf{L}_{\varepsilon n}^T) \quad (4)$$

214 where $vec(\mathbf{E}_n(t))$ is a vector of spatio-temporal variation $\varepsilon_n(s, c, t)$ for all sites s and species c
 215 in a given year t , $\mathbf{L}_{\varepsilon n} \mathbf{L}_{\varepsilon n}^T$ represents the covariance in spatio-temporal variation in numbers
 216 density, and we again define an identical distribution for $\mathbf{E}_w(t)$, involving a separate estimate of
 217 $\mathbf{L}_{\varepsilon w}$. This spatio-temporal index standardization is useful for generating an index of abundance
 218 for each species that has little estimation covariance among years (Thorson 2019b). However, it
 219 does not define a probability distribution for a year with no available data (due to no information
 220 for intercepts in that year).

221 2.2 Extending the model to account for species interactions

222 We next extend this model by defining a probability distribution for population density in
 223 year t given estimates in the previous years. To do so, we approximate nonlinear dynamics for
 224 species interactions via a first-order Taylor series expansion around its equilibrium, which results
 225 in a first-order vector autoregressive model (Ives *et al.* 2003; Thorson *et al.* 2017; Certain *et al.*
 226 2018):

$$\log(\mathbf{d}(s, t)) = \boldsymbol{\alpha}(s) + \mathbf{B} \log(\mathbf{d}(s, t - 1)) + \dots \quad (5)$$

227 where $\boldsymbol{\alpha}(s)$ is a vector of spatially varying and time-invariant intercepts, composed of $\alpha(s, c)$ for
 228 each species c , which represents spatial variation in carrying capacity. \mathbf{B} is the species
 229 interactions matrix where b_{c,c^*} indicates that a 1% change in density for species c^* causes a
 230 change of b_{c,c^*} in per-capita productivity for species c . We parameterize the species-interactions
 231 matrix as:

$$\mathbf{B} = \mathbf{P} + \boldsymbol{\chi} \boldsymbol{\psi}^T \quad (6)$$

232 where \mathbf{P} is a diagonal matrix where diagonal element $\rho(c, c) - 1$ represents intra-specific
 233 density dependence (the degree that population density for species c decreases per-capita

234 productivity for that species), and $\boldsymbol{\chi}\boldsymbol{\psi}^T$ represents inter-species density dependence. $\boldsymbol{\chi}$ and $\boldsymbol{\psi}$ are
 235 both C by R matrices, where the user specifies rank R and this controls the number of interaction
 236 parameters that must be estimated; other identifiability restrictions must be imposed as R
 237 approaches the number of species C , and this parameterization is common in cointegration
 238 models used in econometrics (Engle and Granger 1987; Thorson *et al.* 2017). Importantly, the
 239 user-specified rank of species interactions R can range from 0 to C (i.e., $0 \leq R \leq C$), where the
 240 rank represents the number of ratio-dependent axes of community regulation arising from species
 241 interactions, and where $\boldsymbol{\chi}\boldsymbol{\psi}^T$ can be defined to have either complex or real eigenvalues
 242 (representing dynamics with or without population cycles) depending upon the quality of
 243 available data (Thorson *et al.* 2017).

244 In addition to approximating species interactions via an autoregressive model, we again
 245 include spatial variation (e.g., $\omega_n(s, c)$) and spatio-temporal variation (e.g., $\boldsymbol{\epsilon}_n(s, t)$) and also
 246 incorporate the impact of an instantaneous fishing mortality rate $\mathbf{f}(t)$ on population density:

$$\log(\mathbf{d}(s, t)) = \boldsymbol{\alpha} + \boldsymbol{\omega}(s) + \mathbf{B} \log(\mathbf{d}(s, t - 1)) + \boldsymbol{\epsilon}(s, t) - \mathbf{f}(t) \quad (7)$$

247 Solving for $\log(\mathbf{d}(s, t))$ and re-writing as a delta-model then yields:

$$\log(\mathbf{n}(s, t)) = \boldsymbol{\beta}_n + \boldsymbol{\omega}_n(s) + \sum_{\Delta=0}^t \mathbf{B}^\Delta \boldsymbol{\epsilon}_n(s, t - \Delta) - \xi \sum_{\Delta=0}^t \mathbf{B}^\Delta \mathbf{f}(t - \Delta) \quad (8a)$$

$$\log(\mathbf{w}(s, t)) = \boldsymbol{\beta}_w + \boldsymbol{\omega}_w(s) + \sum_{\Delta=0}^t \mathbf{B}^\Delta \boldsymbol{\epsilon}_w(s, t - \Delta) - (1 - \xi) \sum_{\Delta=0}^t \mathbf{B}^\Delta \mathbf{f}(t - \Delta) \quad (8b)$$

248 where species interactions \mathbf{B} are identical between the two components of the delta model, and
 249 where ξ determines the degree to which fishing mortality decreases numbers density or biomass-
 250 per-individual (we assume $\xi = 1$ in the following, but future research could explore the topic
 251 further). Terms summing across lag Δ , $\sum_{\Delta=0}^t \mathbf{B}^\Delta \boldsymbol{\epsilon}_n(s, t - \Delta)$ and $\sum_{\Delta=0}^t \mathbf{B}^\Delta \mathbf{f}(t - \Delta)$, represent the

252 decaying effect of spatio-temporal variation and fishing mortality, respectively, occurring Δ
253 years previous to year t ; the contribution of previous spatio-temporal variation and fishing
254 mortality is additive due to our model specification, and this specification results in fast
255 computation relative to other model structures. Fishing mortality rate $\mathbf{f}(t)$ must be specified as
256 data for every species, although future research could extend the model to estimate this as a
257 parameter by fitting to fishery catches. The model can also be extended to include catchability
258 covariates, density covariates, and vessel effects that can be incorporated into VAST (see
259 Thorson (2019b) for a description). Although we do not explore these features here (and they
260 would require further software development to be used in conjunction with estimates of species
261 interactions), we recommend future research to incorporate covariates so that, e.g., dynamics
262 could be driven by downscaled climate projections (Hollowed *et al.* 2013).

263 Finally, we calculate biological reference points (BRP) for population abundance and fishing
264 intensity. As BRP for population abundance, we calculate average unfished biomass $b_0(c)$ for
265 each species c and envision a scenario in which fisheries managers seek to maintain a population
266 biomass near a proxy for maximum sustainable yield, $b(c) \approx 0.4b_0(c)$, corresponding to 40% of
267 unfished biomass. We use $b_{40\%}$ as it is used as a proxy biomass target for in other US
268 management regions, e.g., for US West Coast rockfishes (Wetzel *et al.* 2017), and future studies
269 could specify a different target or expand the model to accommodate other proxy reference
270 points (e.g., Gabriel and Mace 1999). As BRP for fishing intensity, we calculate the
271 corresponding fishing mortality rate $f_{0.4}(c)$ that would result in 40% of unfished biomass if
272 $f_{0.4}(c)$ were continued indefinitely (sensu Holsman *et al.* 2016b). Given these BRPs, we then
273 calculate stock status as the ratio of fishing mortality or expected biomass in a given year with
274 the associated BRP; see Appendix A for more details regarding computation.

275 2.3 Parameter estimation

276 We fit this model using a publicly available package VAST (Thorson and Barnett 2017),
277 release number 3.1.0 (<https://github.com/James-Thorson/VAST>) within the R statistical
278 environment (R Core Team 2017). This R package has been used in a variety of different stock
279 and ecosystem assessment reports in several marine regions worldwide (Thorson 2019b) but has
280 not previously included features for estimating species interactions \mathbf{B} , the impact of fishing
281 mortality $\mathbf{f}(t)$, or biological reference points. Species interactions had previously been explored
282 in several recent spatio-temporal models (Ovaskainen *et al.* 2017; Thorson *et al.* 2017; Schliep *et*
283 *al.* 2018), but this study is the first to our knowledge to incorporate both species interactions and
284 fishing mortality in a multispecies spatio-temporal model. We argue that this combination of
285 features represents the minimum necessary for a MICE-in-space model.

286 VAST estimates spatial variation $\boldsymbol{\omega}(s)$ and spatio-temporal variation $\boldsymbol{\epsilon}(s, t)$ for all species,
287 locations, and times as random effects. Users of VAST specify a number of knots n_x , and VAST
288 then uses R package R-INLA (Lindgren and Rue 2013) to generate a triangulated mesh, with
289 vertices at these n_x knots as well as additional boundary vertices, where the total number of
290 knots and boundary vertices is n_s . VAST then estimates spatial variables at all n_s locations,
291 while associating every survey record i with the knot s_i closest to it. Similarly, VAST associates
292 every location in a user-specified extrapolation grid with the knot s_g closest to it. It then uses
293 these predicted values within the extrapolation grid for all plotting and when calculating derived
294 quantities (see the VAST user manual for more details: [https://github.com/James-Thorson-](https://github.com/James-Thorson-NOAA/VAST/blob/master/manual/VAST_model_structure.pdf)
295 [NOAA/VAST/blob/master/manual/VAST_model_structure.pdf](https://github.com/James-Thorson-NOAA/VAST/blob/master/manual/VAST_model_structure.pdf)).

296 VAST estimates parameters by identifying the values that maximize a log-likelihood
297 function. It estimates several fixed effects as defined previously: species interactions matrix \mathbf{B} ,

298 spatial correlations $\mathbf{L}_{\omega n}$, spatio-temporal correlations $\mathbf{L}_{\epsilon n}$, spatial decorrelation rate κ_n ,
299 geometric anisotropy \mathbf{H} , residual sampling variation $\sigma^2(c)$, numbers-density intercepts $\beta_n(c)$
300 and average-weight $\beta_w(c)$ for each species c . To calculate the marginal log-likelihood, it
301 approximates the integral across all random effects using the Laplace approximation (Skaug and
302 Fournier 2006), and specifically integrates across random effects representing spatial variation
303 $\omega(s)$ and spatio-temporal variation $\epsilon(s, t)$ for all species, locations, and times. The Laplace
304 approximation is implemented using package TMB (Kristensen *et al.* 2016), which uses
305 automatic differentiation to efficiently calculate the matrix of second derivatives (used in the
306 Laplace approximation) and the gradient of the Laplace approximation (used when maximizing
307 fixed effects). TMB predicts all random effects by maximizing the joint likelihood function
308 given maximum likelihood estimates of fixed effects, and we use the epsilon bias-correction
309 estimator to correct for “retransformation bias” when predicting any derived quantity (e.g.,
310 biomass biological reference point $b_{ratio}(c, t)$) that involves a nonlinear transformation of
311 predicted random effects (Thorson and Kristensen 2016). TMB also applies a generalization of
312 the delta-method to calculate standard errors for all fixed and random effects, as well as all
313 derived quantities (Kass and Steffey 1989).

314 We note that this MICE-in-space model involves the assumption that the expected survey
315 catches are proportional to local abundance and sample the entire stock. This assumption is
316 analogous to assuming that the catchability coefficient $q = 1$, and this assumption (or variants
317 involving a tight prior) are common in stock assessments in the Gulf of Alaska. Future
318 developments of the MICE-in-space model may involve estimating a catchability coefficient,
319 presumably by treating the fishery history as a depletion experiment as this is the primary source
320 of information in biomass-dynamic models (Magnusson and Hilborn 2007). We leave this as a

321 topic of future development and exploration, but note that our assumptions about catchability
322 result in precise estimates of population scale relative to other model assumptions.

323 **2.4 Case study application**

324 We demonstrate this model via application to data for four commercially important species in
325 the US Gulf of Alaska: Alaska pollock, Pacific cod, Pacific halibut (*Hippoglossus stenolepis*),
326 arrowtooth flounder (*Atheresthes stomias*). We fit the model to biomass-sampling data obtained
327 from a bottom trawl survey data from 1982-2015, conducted every 3rd year from 1982-1999 and
328 every 2nd year from 1999 to present day (Von Szalay and Raring 2016). For fishing mortality,
329 we extract the ratio of fishery catches and stock assessment estimates of total biomass, and
330 define $f(c, t) = -\log(1 - c(c, t)/b(c, t))$.

331 We compare model performance for one descriptive model, and four nested models that
332 incorporate density dependence:

- 333 1. *Index standardization model*: As a descriptive model, we fit a standard “index
334 standardization model” (Eq. 2). We include this model to show estimates of abundance
335 patterns for a “saturated” model that lacks the mechanistic detail of other models.
- 336 2. *Complete density dependence*: As a simplified model that includes density dependence and
337 fishing mortality, we specify a model with “complete” density dependence where spatio-
338 temporal variation and fishing mortality in year t has no impact on values in subsequent
339 years.
- 340 3. *Same density dependence*: Next, we include a model estimating the same degree of density
341 dependence for all species while including fishing mortality, but without estimating
342 interactions.

343 4. *Different density dependence*: We also include a more complex version of model #3 but
344 where density-dependence varies among species, while including fishing mortality but still
345 ignoring interactions.

346 5. *Species interactions*: Finally, we include a model with community-level regulation ($\mathbf{B} =$
347 $\mathbf{P} + \boldsymbol{\chi}\boldsymbol{\psi}^T$, where $\text{rank}(\boldsymbol{\chi}) = 1$ and intra-specific density dependence is identical across
348 species) and fishing mortality. This model is useful to show whether species interactions
349 improves model fit relative to ignoring interactions among species.

350 Models 2-5 are nested and all are intended to bridge continuously from description (model #1) to
351 mechanistic (model #5); see Appendix B for more details.

352 To visualize results, we show log-biomass density at each modeled location and each species:

$$\log(\hat{\mathbf{d}}(s, t)) = \{\boldsymbol{\beta}_n + \boldsymbol{\omega}_n(s) + \boldsymbol{\varepsilon}_n(s, t)\} + \{\boldsymbol{\beta}_w + \boldsymbol{\omega}_w(s) + \boldsymbol{\varepsilon}_w(s, t)\} \quad (12)$$
$$- \left\{ \sum_{\Delta=0}^t \mathbf{B}^\Delta \mathbf{f}(t - \Delta) \right\}$$

353 and where we calculate unfished biomass density $\hat{\mathbf{d}}(s, t_0)$ by fixing $f(c, t_0) = 0$. We
354 recommend future research incorporating dynamic habitat variables (e.g., bottom temperature) as
355 physical drivers of changing productivity, as well as skill-testing for models with and without
356 covariates (Tommasi *et al.* 2017; Thorson 2019b) but do not address the topic further here.

357 2.5 Simulation experiment

358 We also explore model performance using a simulation experiment conditioned upon the most
359 parsimonious model fitted to data for these four species in the Gulf of Alaska. To do so, we (1)
360 generate 100 simulated data sets using a “bootstrap simulator” available within the VAST R
361 package, (2) fit a modified model to each simulated data set, and compare estimates from step #2
362 with known values from step #1. The bootstrap simulator uses the specified model structure and

363 estimated values for all fixed effects, but generates new values for all random effects ($\omega_n(s)$,
364 $\epsilon_n(s, t)$, $\omega_w(s)$, and $\epsilon_w(s, t)$) and then generates new values for biomass-sampling data (\mathbf{b})
365 given those simulated values for random effects. In doing so, it generates new data from the
366 same locations, with the same samples sizes and timing as the original data set, and therefore
367 conditions upon both the estimated parameters (fixed effects) and true sample sizes (timing and
368 frequency of sampling) that is available in the real world while generating new spatial
369 configurations (random effects) for the interacting species.

370 For each simulation replicate, we fit a reduced model comprised of data for only two species
371 (arrowtooth and Alaska pollock) and operating at a coarse spatial resolution (50 knots) relative to
372 the resolution used in the bootstrap simulator (100 knots). We do this for two reasons. First,
373 empirical studies in the real-world will always involve fewer interacting species than the “true”
374 number of interacting species operating in nature, and will also involve a reduced spatial
375 resolution relative to the spatial scale operating in nature. Therefore, reducing the number of
376 species and spatial resolution in the estimation model relative to the operating model ensures that
377 both of these potential sources of bias are present in our simulation experiment, although both
378 sources of bias may be stronger or weaker for other data-generating processes. Second, reducing
379 the spatial resolution and number of species increases the speed of parameter estimation, thereby
380 allowing for an efficient simulation experiment. We choose arrowtooth and Alaska pollock
381 because diet analysis has demonstrated strong predation of arrowtooth upon juvenile Alaska
382 pollock (Gaichas *et al.* 2015; Spies *et al.* 2017; Livingston *et al.* 2017). We then evaluate model
383 fit by comparing estimated and true values for the species interaction matrix \mathbf{B} as well as
384 estimates of the fishing mortality biological reference point $\mathbf{f}_{0.4}$. Based on previous research, we

385 expect that the sign of species interactions should be correctly estimated in the majority of
386 simulation replicates (Thorson *et al.* 2017; Certain *et al.* 2018).

387 **3. Results**

388 Fitting five spatio-temporal models with varying structural complexity to data for four
389 commercial species in the Gulf of Alaska shows that these models estimate similar patterns of
390 biomass (Fig. 1). Specifically, pollock has its highest biomass in 1989 before declining to low
391 biomass in 2001/2007 when fishing mortality rates are relatively high, and Pacific cod similarly
392 reaches its lowest biomass in 2001 before recovering somewhat despite elevated fishing
393 mortality rates. By contrast, arrowtooth flounder attains high biomass in 1989-1992 and again in
394 2003-2005 before declining in recent years. The index-standardization and “perfect density
395 dependence” models only provides estimates of biomass in years with available data, while the
396 other models interpolate biomass between years with sampling data, although uncertainty
397 intervals are wider for years without sampling data (e.g., see the width of uncertainty intervals
398 for arrowtooth flounder in unsampled years 1990/1991 relative to sampled years 1989/1992).

399 Three MICE-in-space models estimate biological reference points, while “index-
400 standardization” and “complete density dependence” models do not. Despite estimating similar
401 patterns in population biomass, these three MICE-in-space models provide different estimates of
402 the fishing mortality rate expected to attain 40% of unfished biomass ($\mathbf{f}_{0.4}$, left column in Fig. 2).
403 The “same density dependence” model by design estimates the same $\mathbf{f}_{0.4}$ for all species, while
404 the “species interactions” model estimates a relatively high $\mathbf{f}_{0.4}$ for pollock and lower $\mathbf{f}_{0.4}$ for
405 other species. The “different density dependence” model also estimates relatively large standard
406 errors for $\mathbf{f}_{0.4}$ (broad distributions in left column Fig. 2). Differences in $\mathbf{b}_{\text{target}}$ estimates for
407 each species are much smaller than differences in $\mathbf{f}_{0.4}$ among models (right column of Fig. 2).

408 Model selection using the Akaike Information Criterion (AIC) suggests that “species
409 interactions” model is the most parsimonious model (Table 1), although the “different density
410 dependence” model also has strong support ($\Delta AIC = 1.0$). The AIC-selected “species
411 interactions” model includes four interactions among species that are significant based on a two-
412 sided Wald test at $p < 0.05$, representing a negative impact of pollock on per-capita productivity
413 of all other species as well as a positive impact of Pacific halibut on productivity of arrowtooth
414 flounder (see Appendix C for these results for the “different density dependence model”).
415 Inspecting estimates of population density from the AIC-selected model with species interactions
416 (Fig. 3), we see, e.g., that arrowtooth flounder has increased in density primarily inshore from
417 Kodiak Island. Similarly, biomass of pollock in 1984 and 1995 is concentrated offshore from
418 Kodiak Island, and the low biomass in 2005 is due in part to decreased density southwest of
419 Kodiak in that period. All three MICE-in-space models that estimate biological reference points
420 show similar trends in stock status, but differ in scale particularly for Pacific halibut and walleye
421 Pollock, due primarily to differences in estimated biological reference points (Fig. 4). The AIC-
422 selected “species interactions” model shows that fishing mortality is above the estimate of $f_{0.4}$
423 for Pacific cod from 2011-2015, while the “different density dependence” model (which also has
424 substantial support) shows fishing mortality slightly below $f_{0.4}$ for those same years; both
425 models estimate that Pacific cod biomass was below 40% of b_0 in 2001 and was approaching
426 that level again by 2015 (Fig. 4). However, stock status is not perfectly correlated between
427 fishing mortality and biomass reference points due to short-term environmental variation,
428 interactions, and other effects that can, e.g., allow biomass to remain above 40% of b_0 despite
429 fishing above $f_{0.4}$. These same factors can cause biomass to exceed average unfished biomass

430 \mathbf{b}_0 for several years, and arrowtooth flounder spends nearly half of the modeled years above this
431 biomass due to process errors and a close-to-zero fishing mortality rate (Fig. 4 top-left panel).

432 Last, we include results from a simulation experiment exploring the ability of a MICE-in-
433 space model to correctly estimate species interactions given plausible forms of model mis-
434 specification, i.e., (1) ignoring species that have non-negligible interactions with modeled
435 species, and (2) modeling dynamics at a coarser spatial resolution than the resolution of
436 biological interactions. To visualize this simulation design, we compare true and estimated
437 population density for a single replicates of the simulation experiment (Fig. 5). This shows that
438 the model can accurately capture spatial variation in unfished population density (i.e., comparing
439 1st and 2nd rows of Fig. 5), as well as density in the final year (3rd and 4th rows of Fig. 5), despite
440 only fitting biomass for two of the four simulated species and fitting density at a coarser spatial
441 scale than is used when simulating data. When summarizing across all simulation replicates, the
442 MICE-in-space model is able to estimate the negative impact of pollock on arrowtooth
443 productivity (Fig. 6A, top-right panel) and the negative impact of arrowtooth on pollock
444 productivity (Fig. 6A, bottom-left panel) in nearly all simulation replicates, although these
445 estimates appear to be biased towards more negative numbers (stronger interactions). Similarly,
446 the majority of simulation replicates estimate a negative impact of arrowtooth on pollock
447 productivity (Fig. 6A, bottom-left panel), and density-dependence (Fig. 6A diagonal panels) are
448 approximately unbiased. The bias in interactions translates to some bias in estimates of fishing
449 mortality reference point for arrowtooth flounder (Fig. 6B top panel), where the MICE-in-space
450 model exhibits a positive bias in $f_{0.4}$ for arrowtooth flounder. However, the majority of
451 simulation replicates correctly identify that arrowtooth has a lower $f_{0.4}$ than pollock. We
452 therefore conclude that, given the quantity and frequency of available data and conditioning the

453 simulation experiment upon estimates from the “species interactions” model, the MICE-in-space
454 model is able to estimate broad qualitative differences in productivity among species as well as
455 the likely sign of species interactions. However, caution should be exercised when interpreting
456 the exact value for fishing mortality targets based on this multispecies model.

457 **4. Discussion**

458 In this paper, we have developed the first multispecies spatio-temporal model that includes
459 species interactions, fishing mortality, and statistical estimates of species-specific biological
460 reference points commonly used for fisheries management. We have showed that a MICE-in-
461 space can function as an operating model within a simulation study, and this simulation
462 experiment suggests that the model can accurately estimate species interactions even in the
463 presence of likely forms of model mis-specification (i.e., missing fine-scale dynamics and
464 modeling only a subset of interacting species). Finally, a case-study demonstration involving
465 four species in the Gulf of Alaska has showed that incorporating species interactions is more
466 parsimonious than assuming independent dynamics among species, although an alternative
467 model with separate density dependence for each species but no interactions had similar support
468 ($\Delta AIC = 1.0$). Various configurations of the model estimated similar trends in biomass and
469 biomass reference points but differed more in estimated fishing mortality reference points, and
470 this is in-line with other previous multi-species model comparisons (Kinzey and Punt 2009;
471 Holsman *et al.* 2016b).

472 The species interactions estimated from MICE-in-space contrast with previous analyses of
473 trophic relationships based on diet analyses in the Gulf of Alaska. Models that include diet data
474 suggest that arrowtooth flounder, cod, and halibut account for the majority of predation upon
475 pollock (Gaichas *et al.* 2015) and therefore predict that these stocks have a negative impact on

476 pollock productivity (A'mar *et al.* 2010; Van Kirk *et al.* 2010). However, the MICE-in-space
477 developed here estimated no significant impact of either arrowtooth flounder, cod, or halibut on
478 pollock productivity. Previous ecosystem models have also suggested that increased pollock
479 production would lead to increased halibut production (Gaichas *et al.* 2015), in contrast with the
480 negative impact of pollock on halibut estimated here.

481 Diet data represent the integrated outcome of behavioral and spatial processes that underlie
482 variation in consumption across habitats, years, species, and individuals. Diet studies therefore
483 provide valuable information regarding trophic interactions that structure marine ecosystems
484 (e.g., Livingston *et al.* 2017). However, estimates of predation impacts on species productivity
485 will typically depend upon structural modelling assumptions, such that models may differ about
486 the magnitude or sign of species interactions even when fitting to diet data (Kaplan *et al.* 2018;
487 Reum *et al.* 2019). Finally, non-consumptive processes may cause diet analyses to misrepresent
488 the cumulative impact of changing biomass for one species on per-capita productivity for other
489 species. For example, behavioral plasticity can reduce foraging rates in many species (e.g.,
490 Heithaus *et al.* 2007), resulting in a decrease in productivity (due to decreased weight-at-age)
491 that exceeds that predicted due to a direct change in natural mortality measured by predator
492 stomach contents. Comparing results from multiple ecosystem models can help to evaluate the
493 sensitivity of estimated ecosystem properties to structural assumptions and multiple data sources.
494 We therefore support ongoing comparative research using multiple ecological models when
495 evaluating climate or human-mediated changes on marine ecosystems (Olsen *et al.* 2016; Kaplan
496 *et al.* 2018; Spence *et al.* 2018; Tittensor *et al.* 2018; Pope *et al.* 2019), and note that the MICE-
497 in-space model could fill a useful niche in these model portfolios.

498 Given the differences in estimated interactions between the MICE-in-space model and
499 previous ecosystem models using diet-data, we do not recommend using the MICE-in-space
500 model for analyzing harvest trade-offs between species in the Gulf of Alaska (e.g., Walters *et al.*
501 2005; Moffitt *et al.* 2016) until these differences have been explained and addressed. However,
502 we note that the MICE-in-space model estimates fine-scaled variation in multispecies density,
503 and also discriminates species interactions from the covariance caused by different responses to
504 shared but unmeasured environmental drivers. We therefore believe that the MICE-in-space
505 model is ready for use for several real-world fisheries management activities including projection
506 of localized climate impacts, optimization of survey designs, designation of essential fish habitat,
507 and multi-model inference regarding fishery status and productivity. We discuss each of these in
508 detail below.

509 **4.1 Projecting climate impacts**

510 Globally, marine heatwaves of anomalously warm conditions are increasing in frequency and
511 strength (Hobday *et al.* 2016a). Climate-driven changes to the survival and distribution of
512 species are have also been well documented (Pinsky *et al.* 2013; Alabia *et al.* 2018; Morley *et al.*
513 2018). Rapid reorganization of food webs, novel interactions, and shifting spatial distributions
514 confound traditional assessment methods that do not consider unidirectional change or non-
515 stationarity in environmental drivers of mortality, selectivity, and growth (Skern-Mauritzen *et al.*
516 2015; Pinsky *et al.* 2018). As such, future short-term forecasts and long-term projections of
517 many fish stocks will likely require models that include climate-driven changes to spatial
518 distributions and species interactions (Deyle *et al.* 2016; Hobday *et al.* 2016b, 2018; Tommasi *et al.*
519 *et al.* 2017). Spatially-explicit MICE models such as the one presented here represent a potential
520 tool for managing fisheries under changing conditions, as they can be used to forecast changes in

521 spatial distribution while accounting for species interactions (Howell and Filin 2014).
522 Presumably, skillful forecasting over longer time-horizons (e.g., >10 years) will require
523 including incorporating physiological and other mechanistic processes (Hollowed *et al.* 2009;
524 Payne *et al.* 2017); we recommend future research to explore including density covariates
525 representing changes in thermal niche, as well as the effect of regional oceanographic variables
526 (Thorson 2019) within MICE-in-space models.

527 **4.2 Optimizing survey designs**

528 In addition to potential conflict between governments (Pinsky *et al.* 2018), changing spatial
529 distributions due to climate change complicates fisheries management because historical survey
530 operations and methods may no longer cover the range of important fish populations (Karp *et al.*
531 In press). For example, walleye pollock and Pacific cod in the Bering Sea are enormously
532 productive and valuable fisheries, and both shifted northward out of the historically surveyed
533 area between 2010 and 2017 (Stevenson and Lauth 2019). Fisheries science and management
534 agencies therefore face a difficult task of funding existing resource surveys versus developing
535 new surveys in response to changes in resource distribution and productivity. Existing fishery-
536 independent surveys are often very expensive (e.g., approximately \$1 million US for vessel time
537 alone for the 130 bottom trawl stations in the northern Bering Sea in 2017) and agencies face
538 trade-offs between decreased survey sample sizes or frequency in existing surveys vs. extending
539 surveys to new areas. The trade-off between maintaining existing surveys and developing new
540 ones would ideally be informed by scientific methods that condition upon available data and
541 incorporate known and/or hypothesized forms of spatial, temporal, and sampling variation (e.g.,
542 Reich *et al.* 2018). Similarly, changing ocean use (e.g., offshore energy development) can
543 impact survey design, and it would be helpful to understand likely impacts of these

544 developments on existing survey performance. We therefore recommend future research using a
545 MICE-in-space model for survey evaluation and optimization, whereby a MICE-in-space
546 operating model is fitted to available historical data for interacting species (given their historical
547 fishing mortality rates) to generate simulated sampling data under alternative potential sampling
548 designs. Each simulated data set could then be fitted by each sampling design, and the average
549 performance (e.g., standard error when estimating an index of abundance, or the strength of
550 species interactions) could be calculated across all simulation replicates. This method would
551 represent an objective process to evaluate alternative configurations of limited sampling effort,
552 and could presumably result in more efficient use of limited agency sampling, although it would
553 be unlikely to capture the additional value of sampling data under environmental conditions that
554 have not previously been observed.

555 **4.3 Designation of essential fish habitat**

556 Fisheries managers use a wide array of spatial management tools in addition to regulations on
557 fishery catch, effort, timing, and gear. In the US, fisheries management councils are required to
558 update designations of essential fish habitat (EFH) and habitat areas of particular concern
559 (HAPC) every five years. These designations can be done using species distribution models,
560 SDMs (Rooper *et al.* 2016), and the MICE-in-space is a generalization of these models that
561 additionally includes fishery harvest, species co-occurrence, and biological interactions. We
562 note that the US national EFH program defines four levels of EFH model (NMFS 2010;
563 Lederhouse *et al.* 2017), ranging from low (Levels 1-2: population distribution and density) to
564 high (Levels 3-4: spatial variation in demographic rates and overall productivity). Within this
565 classification, a MICE-in-space reconstructs spatial variation in productivity from survey
566 biomass and fishery removals, and therefore represents the highest-level basis for designating

567 EFH. Unlike previous EFH models, however, the MICE-in-space estimates temporal variability
568 in species distribution, density, and productivity, driven by both species interactions, fishing, and
569 residual spatio-temporal variation. Temporal variability has not been extensively addressed in
570 EFH models or processes in the US, although we note that EFH-designations are already updated
571 every 5 years and could be designated using five-year forecasts of productivity given forecasted
572 environmental conditions. However, whether this time-varying designation of EFH and HAPC
573 is acceptable to stakeholders and fisheries managers will of course depend upon many local and
574 non-technical considerations including: available human resources; management priorities; and
575 previous regional approaches to EFH designation (Copps *et al.* 2007).

576 **4.4 Multi-model inference regarding status and productivity**

577 Non-spatial climate-enhanced multispecies models (Holsman *et al.* 2016b), and climate-
578 enhanced single-species models (Spencer *et al.* 2016; Barbeaux *et al.* 2017) are increasingly
579 evaluated for Alaskan stocks impacted by anomalously warm conditions in the North Pacific.
580 Balancing model complexity and mechanistic detail with computational demand, data
581 compilation, and ease of interpretation of results is an ongoing challenge, especially for models
582 that require multiple data sources and types (Plagányi *et al.* 2011). Stepwise hierarchical
583 selection approaches for narrowing the focal components for forecasting risk can help balance
584 demands and costs in computing, and identify key attributes to be evaluated in MICE models,
585 which are intermediate in complexity but represent highly quantitative approaches (Hobday *et al.*
586 2011; Holsman *et al.* 2017). Shifting spatial distributions and changing mortality rates (e.g.,
587 through predation or starvation) are often confounded in ecosystem models, and simultaneously
588 addressing these two issues is a key goal in current ecosystem models in regions including the
589 Bering Sea (e.g., Spencer *et al.* 2016). Underlying model structure and implicit versus explicit

590 treatment of environmental or trophic changes to a population becomes extremely important
591 when projecting models for management advice, especially on longer timescales (Lotze *et al.*
592 2019). Forecasting distribution and productivity using a wide range of models with different
593 structural assumptions (a.k.a. multi-model inference) can be used to identify sensitivities in
594 model specification and propagation of error (Kaplan *et al.* 2018; Spence *et al.* 2018; Pope *et al.*
595 2019). Examples of this multi-model approach to forecasting climate impacts include FISH-MIP
596 (Hobday *et al.* 2016b; Tittensor *et al.* 2018) and the Alaska Climate Change Integrated Modeling
597 project (ACLIM; Hollowed *et al.* submitted). We recommend further research regarding MICE-
598 in-space models when used within an ensemble of other models that have less spatial resolution
599 but more detailed submodels for population demography (e.g., age or size structure) or physical
600 drivers (e.g., linked to regional biophysical models, e.g., Hermann *et al.* (In press)).

601 **4.5 Future research**

602 We recommend several avenues for future research regarding MICE-in-space, including: (1)
603 incorporating prior information regarding species interactions; (2) fitting to fishery catches; (3)
604 incorporating density covariates; and (4) comparison with alternative ecosystem models.

605 1. *Prior information regarding species interactions*: In this paper, we have freely estimated
606 species interactions given information in survey data. However, analysts could seek to
607 incorporate prior information (e.g., from diet data or assumptions about bioenergetics), and
608 we envision two ways to do so. First, analysts could “hardwire” the interaction matrix, either
609 eliminating some interactions a priori (e.g., Rochet *et al.* 2011) or such that it matches
610 specified values for single-species intrinsic growth rates and per-capita consumption rates.
611 Alternatively, analysts might specify a Bayesian prior on these values while using available

612 data. The latter would require additional statistical research, but would allow analysts to
613 integrate diet analyses while retaining the computational flexibility of the current study.

614 2. *Fitting to fishery catches*: In this paper, we have pre-specified a fishing mortality rate for
615 each species that varies among years but is constant across space, and this has driven
616 interannual variation in status relative to estimated biological reference points. We again see
617 two ways to relax this assumption. First, analysts could specify spatial variation in fishing
618 mortality, such that forecasts incorporate historical data regarding the spatial distribution of
619 fishing effort. Alternatively, analysts could specify spatial variation in fishery catch or
620 landings (obtained from fishery observers or other reporting). Specifying fishery catch for
621 each species, location, and year would require estimating fishing mortality rates as a model
622 parameter, but this specification would still be “separable” and previous exploration suggests
623 that this could be done while still being computationally feasible. Neither of these options
624 are currently available in the R package VAST used here, but both could be added during
625 future developments.

626 3. *Incorporating density covariates*: Forecasting climate impacts is a growing concern for
627 identifying suitable management strategies (Miller *et al.* 2010; Holsman *et al.* 2019a).
628 Covariates explaining historical variation in density will improve predictive skill for short-
629 term forecasts in some cases and not others (Hobday *et al.* 2018; Thorson 2019a), so we
630 encourage future skill-testing to measure the potential benefits of incorporating multi-species
631 interactions, density covariates, and species associations for forecasting distribution shifts
632 over short (<3 year) or longer time-horizons.

633 4. *Comparison with alternative ecosystem models*: Perhaps most importantly, we recommend
634 detailed, side-by-side comparison of MICE-in-space and other ecosystem models. These

635 comparisons are vital to identify the relative computational and human-resource costs of
636 these different models, as well as identify when models provide different advice (Kaplan *et*
637 *al.* 2018; Pope *et al.* 2019). However, this topic would require substantial additional effort
638 and is an obvious topic for future research.

639 The MICE-in-space is publicly available in the R package *VAST*, which is already used for stock
640 assessment and ecosystem status reports in the North Pacific (Thorson 2019b). We anticipate
641 that public access and ongoing documentation for this implementation of a “MICE-in-space”
642 model will facilitate future model comparisons. We hope that it will facilitate the use of
643 multispecies models for spatial management including climate forecasts, survey optimization,
644 and EFH designation.

645 **Data Availability Statement**

646 All data used are publicly available and hosted by the Alaska Fisheries Science Center. Survey
647 data can be accessed online at http://www.afsc.noaa.gov/RACE/groundfish/survey_data/data.htm
648 and records of fishing mortality are online at
649 https://www.afsc.noaa.gov/REFM/Stocks/SARA/sara_access.php. The R package *VAST* is
650 available at <https://github.com/James-Thorson/VAST/>.

651 **Acknowledgements**

652 We thank K. Aydin for discussions while developing ideas in this project, and I. Kaplan, K.
653 Aydin, and two anonymous reviewers for comments on a previous draft. We also thank K.
654 Kristensen and the developers of Template Model Builder, the many people who have
655 contributed to the development and testing of package *VAST*, and acknowledge support from a
656 grant #15-027 from the Habitat Assessment Improvement Plan to develop and document the
657 earlier package *SpatialDeltaGLMM*. Finally, we thank the many scientists who have contributed

658 to the Gulf of Alaska Bottom Trawl Survey, which is an invaluable resource for studying that
659 region.

660

661 **References**

- 662 Alabia, I.D., García Molinos, J., Saitoh, S.-I., Hirawake, T., Hirata, T. and Mueter, F.J. (2018) Distribution
663 shifts of marine taxa in the Pacific Arctic under contemporary climate changes. *Diversity and*
664 *Distributions*, 1–15. doi:10.1111/ddi.12788.
- 665 A’mar, Z.T., Punt, A.E. and Dorn, M.W. (2010) Incorporating ecosystem forcing through predation into a
666 management strategy evaluation for the Gulf of Alaska walleye pollock (*Theragra*
667 *chalcogramma*) fishery. *Fisheries Research* **102**, 98–114. doi:10.1016/j.fishres.2009.10.014.
- 668 Barbeaux, S., Aydin, K., Fissel, B., et al. (2017) Assessment of the Pacific cod stock in the Gulf of Alaska.
669 *NPFMC Gulf of Alaska SAFE*, 183–326.
- 670 Begley, J. and Howell, D. (2004) An overview of Gadget, the globally applicable area-disaggregated
671 general ecosystem toolbox. ICES.
- 672 Berger, A.M., Goethel, D.R., Lynch, P.D., Quinn, T., Mormede, S., McKenzie, J. and Dunn, A. (2017) Space
673 oddity: The mission for spatial integration. *Canadian Journal of Fisheries and Aquatic Sciences*
674 **74**, 1698–1716. doi:10.1139/cjfas-2017-0150.
- 675 Burnham, K.P. and Anderson, D. (2002) *Model Selection and Multi-Model Inference*, 2nd edn. Springer,
676 New York.
- 677 Certain, G., Barraquand, F. and Gårdmark, A. (2018) How do MAR(1) models cope with hidden
678 nonlinearities in ecological dynamics? *Methods in Ecology and Evolution* **9**, 1975–1995.
679 doi:10.1111/2041-210X.13021.
- 680 Christensen, V. and Walters, C.J. (2004) Ecopath with Ecosim: methods, capabilities and limitations.
681 *Ecological Modelling* **172**, 109–139. doi:10.1016/j.ecolmodel.2003.09.003.
- 682 Collie, J.S., Botsford, L.W., Hastings, A., et al. (2016) Ecosystem models for fisheries management:
683 Finding the sweet spot. *Fish and Fisheries* **17**, 101–125. doi:10.1111/faf.12093.
- 684 Collie, J.S. and Gislason, H. (2001) Biological reference points for fish stocks in a multispecies context.
685 *Canadian Journal of Fisheries and Aquatic Sciences* **58**, 2167–2176.
- 686 Copps, S.L., Yoklavich, M.M., Parkes, G.B., et al. (2007) Applying marine habitat data to fishery
687 management on the US West Coast: Initiating a policy-science feedback loop. *Mapping the*
688 *seafloor for habitat characterization. Geol. Assoc. Can. Spec. Pap* **47**, 451–462.
- 689 Cressie, N. and Wikle, C.K. (2011) *Statistics for spatio-temporal data*. John Wiley & Sons, Hoboken, New
690 Jersey.
- 691 Deyle, E.R., May, R.M., Munch, S.B. and Sugihara, G. (2016) Tracking and forecasting ecosystem
692 interactions in real time. *Proceedings of the Royal Society B: Biological Sciences* **283**.
693 doi:10.1098/rspb.2015.2258.
- 694 Dolan, T.E., Patrick, W.S. and Link, J.S. (2016) Delineating the continuum of marine ecosystem-based
695 management: a US fisheries reference point perspective. *ICES Journal of Marine Science: Journal*
696 *du Conseil* **73**, 1042–1050. doi:10.1093/icesjms/fsv242.
- 697 Dolder, P.J., Thorson, J.T. and Minto, C. (2018) Spatial separation of catches in highly mixed fisheries.
698 *Scientific Reports* **8**, 13886. doi:10.1038/s41598-018-31881-w.
- 699 Engle, R.F. and Granger, C.W. (1987) Co-integration and error correction: representation, estimation,
700 and testing. *Econometrica: journal of the Econometric Society*, 251–276.
- 701 Foster, S.D. and Bravington, M.V. (2013) A Poisson–Gamma model for analysis of ecological non-
702 negative continuous data. *Environmental and Ecological Statistics* **20**, 533–552.
703 doi:10.1007/s10651-012-0233-0.
- 704 Fu, C., Olsen, N., Taylor, N., et al. (2017) Spatial and temporal dynamics of predator-prey species
705 interactions off western Canada. *ICES Journal of Marine Science* **74**, 2107–2119.
706 doi:10.1093/icesjms/fsx056.

707 Fuglstad, G.-A., Lindgren, F., Simpson, D. and Rue, H. avarð (2015) Exploring a new class of non-
708 stationary spatial Gaussian random fields with varying local anisotropy. *Statistica Sinica*, 115–
709 133.

710 Fulton, E.A., Link, J.S., Kaplan, I.C., et al. (2011) Lessons in modelling and management of marine
711 ecosystems: the Atlantis experience. *Fish and Fisheries* **12**, 171–188. doi:10.1111/j.1467-
712 2979.2011.00412.x.

713 Gabriel, W.L. and Mace, P.M. (1999) A review of biological reference points in the context of the
714 precautionary approach. In: *Proceedings of the fifth national NMFS stock assessment workshop:
715 providing scientific advice to implement the precautionary approach under the Magnuson-
716 Stevens fishery conservation and management act. NOAA Tech Memo NMFS-F/SPO-40*. pp 34–
717 45.

718 Gaichas, Aydin, K. and Francis, R.C. (2015) Wasp waist or beer belly? Modeling food web structure and
719 energetic control in Alaskan marine ecosystems, with implications for fishing and environmental
720 forcing. *Progress in Oceanography* **138**, 1–17. doi:10.1016/j.pocean.2015.09.010.

721 Gaichas, S.K., Aydin, K.Y. and Francis, R.C. (2010) Using food web model results to inform stock
722 assessment estimates of mortality and production for ecosystem-based fisheries management.
723 *Canadian Journal of Fisheries and Aquatic Sciences* **67**, 1490–1506. doi:10.1139/F10-071.

724 Heithaus, M.R., Frid, A., Wirsing, A.J., et al. (2007) State-dependent risk-taking by green sea turtles
725 mediates top-down effects of tiger shark intimidation in a marine ecosystem. *Journal of Animal
726 Ecology* **76**, 837–844. doi:10.1111/j.1365-2656.2007.01260.x.

727 Hermann, A.J., Gibson, G.A., Cheng, W., et al. (In press) Projected biophysical conditions of the Bering
728 Sea to 2100 under multiple emission scenarios. *ICES Journal of Marine Science*.
729 doi:10.1093/icesjms/fsz043.

730 Hobday, A.J., Alexander, L. V., Perkins, S.E., et al. (2016a) A hierarchical approach to defining marine
731 heatwaves. *Progress in Oceanography* **141**, 227–238. doi:10.1016/j.pocean.2015.12.014.

732 Hobday, A.J., Cochrane, K., Downey-Breedt, N., et al. (2016b) Planning adaptation to climate change in
733 fast-warming marine regions with seafood-dependent coastal communities. *Reviews in Fish
734 Biology and Fisheries* **26**, 249–264. doi:10.1007/s11160-016-9419-0.

735 Hobday, A.J., Smith, A.D.M., Stobutzki, I.C., et al. (2011) Ecological risk assessment for the effects of
736 fishing. *Fisheries Research* **108**, 372–384. doi:10.1016/j.fishres.2011.01.013.

737 Hobday, A.J., Spillman, C.M., Eveson, J.P., Hartog, J.R., Zhang, X. and Brodie, S. (2018) A Framework for
738 Combining Seasonal Forecasts and Climate Projections to Aid Risk Management for Fisheries and
739 Aquaculture. *Frontiers in Marine Science* **5**, 1–9. doi:10.3389/fmars.2018.00137.

740 Hollowed, A. (2000) Are multispecies models an improvement on single-species models for measuring
741 fishing impacts on marine ecosystems? *ICES Journal of Marine Science* **57**, 707–719.
742 doi:10.1006/jmsc.2000.0734.

743 Hollowed, A.B., Barange, M., Beamish, R.J., et al. (2013) Projected impacts of climate change on marine
744 fish and fisheries. *ICES Journal of Marine Science* **70**, 1023–1037. doi:10.1093/icesjms/fst081.

745 Hollowed, A.B., Bond, N.A., Wilderbuer, T.K., et al. (2009) A framework for modelling fish and shellfish
746 responses to future climate change. *ICES Journal of Marine Science* **66**, 1584–1594.
747 doi:10.1093/icesjms/fsp057.

748 Holsman, K., Samhour, J., Cook, G., et al. (2017) An ecosystem-based approach to marine risk
749 assessment. *Ecosystem Health and Sustainability* **3**, e01256. doi:10.1002/ehs2.1256.

750 Holsman, K.K., Hazen, E.L., Haynie, A., et al. (2019a) Towards climate resiliency in fisheries management.
751 *ICES Journal of Marine Science*. doi:10.1093/icesjms/fsz031.

752 Holsman, K.K., Ianelli, J., Aydin, K., Punt, A.E. and Moffitt, E.A. (2016b) A comparison of fisheries
753 biological reference points estimated from temperature-specific multi-species and single-species

754 climate-enhanced stock assessment models. *Deep Sea Research Part II: Topical Studies in*
755 *Oceanography*. doi:10.1016/j.dsr2.2015.08.001.

756 Howell, D. and Filin, A.A. (2014) Modelling the likely impacts of climate-driven changes in cod-capelin
757 overlap in the Barents Sea. *ICES Journal of Marine Science* **71**, 72–80.
758 doi:10.1093/icesjms/fst172.

759 Hunsicker, M.E., Ciannelli, L., Bailey, K.M., et al. (2011) Functional responses and scaling in predator–
760 prey interactions of marine fishes: contemporary issues and emerging concepts. *Ecology Letters*
761 **14**, 1288–1299. doi:10.1111/j.1461-0248.2011.01696.x.

762 Ives, A.R., Dennis, B., Cottingham, K.L. and Carpenter, S.R. (2003) Estimating community stability and
763 ecological interactions from time-series data. *Ecological monographs* **73**, 301–330.

764 Kaplan, I.C., Francis, T.B., Punt, A.E., et al. (2018) A multi-model approach to understanding the role of
765 Pacific sardine in the California Current food web. *Marine Ecology Progress Series*.

766 Karp, M.A., Peterson, J.O., Lynch, P.D., et al. (In press) Accounting for shifting distributions and changing
767 productivity in the development of scientific advice for fishery management. *ICES Journal of*
768 *Marine Science*. doi:10.1093/icesjms/fsz048.

769 Kass, R.E. and Steffey, D. (1989) Approximate bayesian inference in conditionally independent
770 hierarchical models (parametric empirical bayes models). *Journal of the American Statistical*
771 *Association* **84**, 717–726. doi:10.2307/2289653.

772 Kempf, A., Huse, G., Dingsør, G., Floeter, J. and Temming, A. (2010) The importance of overlap –
773 predicting North Sea cod recovery with a multi species fisheries assessment model. *ICES Journal*
774 *of Marine Science* **67**, 1989–1997.

775 Kinzey, D. and Punt, A.E. (2009) Multispecies and Single-Species Models of Fish Population Dynamics:
776 Comparing Parameter Estimates. *Natural Resource Modeling* **22**, 67–104. doi:10.1111/j.1939-
777 7445.2008.00030.x.

778 Kristensen, K., Nielsen, A., Berg, C.W., Skaug, H. and Bell, B.M. (2016) TMB: Automatic Differentiation
779 and Laplace Approximation. *Journal of Statistical Software* **70**, 1–21. doi:10.18637/jss.v070.i05.

780 Kristensen, K., Thygesen, U.H., Andersen, K.H. and Beyer, J.E. (2014) Estimating spatio-temporal
781 dynamics of size-structured populations. *Canadian Journal of Fisheries and Aquatic Sciences* **71**,
782 326–336. doi:10.1139/cjfas-2013-0151.

783 Lassen, H., Pedersen, S.A., Frost, H. and Hoff, A. (2013) Fishery management advice with ecosystem
784 considerations. *ICES Journal of Marine Science* **70**, 471–479. doi:10.1093/icesjms/fss208.

785 Lindgren, F. and Rue, H. (2013) Bayesian spatial and spatiotemporal modelling with r-inla. *Journal of*
786 *Statistical Software*.

787 Livingston, P.A., Aydin, K., Buckley, T.W., Lang, G.M., Yang, M.-S. and Miller, B.S. (2017) Quantifying food
788 web interactions in the North Pacific – a data-based approach. *Environmental Biology of Fishes*
789 **100**, 443–470. doi:10.1007/s10641-017-0587-0.

790 Lotze, H.K., Tittensor, D.P., Bryndum-Buchholz, A., et al. (2019) Global ensemble projections reveal
791 trophic amplification of ocean biomass declines with climate change. *Proceedings of the*
792 *National Academy of Sciences* **116**, 12907–12912. doi:10.1073/pnas.1900194116.

793 Mackinson, S., Platts, M., Garcia, C. and Lynam, C. (2018) Evaluating the fishery and ecological
794 consequences of the proposed North Sea multi-annual plan. *PLOS ONE* **13**, e0190015.
795 doi:10.1371/journal.pone.0190015.

796 Magnusson, A. and Hilborn, R. (2007) What makes fisheries data informative? *Fish and Fisheries* **8**, 337–
797 358.

798 Magnusson, A., Punt, A.E. and Hilborn, R. (2013) Measuring uncertainty in fisheries stock assessment:
799 the delta method, bootstrap, and MCMC. *Fish and Fisheries* **14**, 325–342.

800 Marshall, K.N., Duffy-Anderson, J.T., Ward, E.J., Anderson, S.C., Hunsicker, M.E. and Williams, B.C. (2019)
801 Long-term trends in ichthyoplankton assemblage structure, biodiversity, and synchrony in the

802 Gulf of Alaska and their relationships to climate. *Progress in Oceanography* **170**, 134–145.
803 doi:10.1016/j.pocean.2018.11.002.

804 Miller, K., Charles, A., Barange, M., et al. (2010) Climate change, uncertainty, and resilient fisheries:
805 Institutional responses through integrative science. *Progress in Oceanography* **87**, 338–346.
806 doi:10.1016/j.pocean.2010.09.014.

807 Moffitt, E.A., Punt, A.E., Holsman, K., Aydin, K.Y., Ianelli, J.N. and Ortiz, I. (2016) Moving towards
808 ecosystem-based fisheries management: Options for parameterizing multi-species biological
809 reference points. *Deep Sea Research Part II: Topical Studies in Oceanography* **134**, 350–359.
810 doi:10.1016/j.dsr2.2015.08.002.

811 Morley, J.W., Selden, R.L., Latour, R.J., Frölicher, T.L., Seagraves, R.J. and Pinsky, M.L. (2018) Projecting
812 shifts in thermal habitat for 686 species on the North American continental shelf. *PLoS ONE* **13**,
813 1–28. doi:10.1371/journal.pone.0196127.

814 Olsen, E., Fay, G., Gaichas, S., Gamble, R., Lucey, S. and Link, J.S. (2016) Ecosystem Model Skill
815 Assessment. Yes We Can! *PLOS ONE* **11**, e0146467. doi:10.1371/journal.pone.0146467.

816 Ortiz, I., Aydin, K., Hermann, A.J., et al. (2016) Climate to fish: Synthesizing field work, data and models
817 in a 39-year retrospective analysis of seasonal processes on the eastern Bering Sea shelf and
818 slope. *Deep-Sea Research Part II: Topical Studies in Oceanography* **134**, 390–412.
819 doi:10.1016/j.dsr2.2016.07.009.

820 Ovaskainen, O., Tikhonov, G., Dunson, D., Grøtan, V., Engen, S., Sæther, B.-E. and Abrego, N. (2017) How
821 are species interactions structured in species-rich communities? A new method for analysing
822 time-series data. *Proc. R. Soc. B* **284**, 20170768. doi:10.1098/rspb.2017.0768.

823 Payne, M.R., Hobday, A.J., MacKenzie, B.R., et al. (2017) Lessons from the First Generation of Marine
824 Ecological Forecast Products. *Frontiers in Marine Science* **4**. doi:10.3389/fmars.2017.00289.

825 Pikitch, E.K., Rountos, K.J., Essington, T.E., et al. (2014) The global contribution of forage fish to marine
826 fisheries and ecosystems. *Fish and Fisheries* **15**, 43–64. doi:10.1111/faf.12004.

827 Pinsky, M.L., Worm, B., Fogarty, M.J., Sarmiento, J.L. and Levin, S.A. (2013) Marine taxa track local
828 climate velocities. *Science* **341**, 1239–1242. doi:10.1126/science.1239352.

829 Plagányi, É.E. (2007) *Models for an ecosystem approach to fisheries*. Food & Agriculture Org.

830 Plagányi, É.E., Bell, J.D., Bustamante, R.H., et al. (2011) Modelling climate-change effects on Australian
831 and Pacific aquatic ecosystems: a review of analytical tools and management implications.
832 *Marine and Freshwater Research* **62**, 1132–1147. doi:10.1071/MF10279.

833 Plagányi, É.E. and Butterworth, D.S. (2012) The Scotia Sea krill fishery and its possible impacts on
834 dependent predators: Modeling localized depletion of prey. *Ecological Applications* **22**, 748–761.
835 doi:10.1890/11-0441.1.

836 Plagányi, É.E., Punt, A.E., Hillary, R., et al. (2014) Multispecies fisheries management and conservation:
837 Tactical applications using models of intermediate complexity. *Fish and Fisheries* **15**, 1–22.
838 doi:10.1111/j.1467-2979.2012.00488.x.

839 Pollock, L.J., Tingley, R., Morris, W.K., et al. (2014) Understanding co-occurrence by modelling species
840 simultaneously with a Joint Species Distribution Model (JSDM). *Methods in Ecology and*
841 *Evolution* **5**, 397–406. doi:10.1111/2041-210X.12180.

842 Pope, J.G., Bartolino, V., Kulatska, N., et al. (2019) Comparing the steady state results of a range of
843 multispecies models between and across geographical areas by the use of the jacobian matrix of
844 yield on fishing mortality rate. *Fisheries Research* **209**, 259–270.
845 doi:10.1016/j.fishres.2018.08.011.

846 R Core Team (2017) *R: A Language and Environment for Statistical Computing*. R Foundation for
847 Statistical Computing, Vienna, Austria.

848 Reich, B.J., Pacifici, K. and Stallings, J.W. (2018) Integrating auxiliary data in optimal spatial design for
849 species distribution modelling. *Methods in Ecology and Evolution* **9**, 1626–1637.
850 doi:10.1111/2041-210X.13002.

851 Reum, J.C.P., Blanchard, J.L., Holsman, K.K., Aydin, K. and Punt, A.E. (2019) Species-specific ontogenetic
852 diet shifts attenuate trophic cascades and lengthen food chains in exploited ecosystems. *Oikos*
853 **0**. doi:10.1111/oik.05630.

854 Rochet, M.-J., Collie, J.S., Jennings, S. and Hall, S.J. (2011) Does selective fishing conserve community
855 biodiversity? Predictions from a length-based multispecies model. *Canadian Journal of Fisheries*
856 *and Aquatic Sciences* **68**, 469–486. doi:10.1139/F10-159.

857 Rooper, C.N., Sigler, M.F., Goddard, P., et al. (2016) Validation and improvement of species distribution
858 models for structure-forming invertebrates in the eastern Bering Sea with an independent
859 survey. *Marine Ecology Progress Series* **551**, 117–130. doi:10.3354/meps11703.

860 Schliep, E.M., Lany, N.K., Zarnetske, P.L., Schaeffer, R.N., Orians, C.M., Orwig, D.A. and Preisser, E.L.
861 (2018) Joint species distribution modelling for spatio-temporal occurrence and ordinal
862 abundance data. *Global Ecology and Biogeography* **27**, 142–155. doi:10.1111/geb.12666.

863 Shin, Y.-J. and Cury, P. (2001) Exploring fish community dynamics through size-dependent trophic
864 interactions using a spatialized individual-based model. *Aquatic Living Resources* **14**, 65–80.
865 doi:10.1016/S0990-7440(01)01106-8.

866 Skaug, H. and Fournier, D. (2006) Automatic approximation of the marginal likelihood in non-Gaussian
867 hierarchical models. *Computational Statistics & Data Analysis* **51**, 699–709.

868 Spence, M.A., Blanchard, J.L., Rossberg, A.G., et al. (2018) A general framework for combining ecosystem
869 models. *Fish and Fisheries* **19**, 1031–1042. doi:10.1111/faf.12310.

870 Spencer, P.D., Holsman, K.K., Zador, S., Bond, N.A., Mueter, F.J., Hollowed, A.B. and Ianelli, J.N. (2016)
871 Modelling spatially dependent predation mortality of eastern Bering Sea walleye pollock, and its
872 implications for stock dynamics under future climate scenarios. *ICES Journal of Marine Science:*
873 *Journal du Conseil* **73**, 1330–1342. doi:10.1093/icesjms/fsw040.

874 Spies, I., Aydin, K., Ianelli, J.N. and Palsson, W. (2017) 7. Assessment of the arrowtooth flounder stock in
875 the Gulf of Alaska. In: *Stock assessment and fishery evaluation report for the groundfish fisheries*
876 *of the Gulf of Alaska*. North Pacific Fishery Management Council, Seattle, WA, pp 743–840.

877 Stevenson, D.E. and Lauth, R.R. (2019) Bottom trawl surveys in the northern Bering Sea indicate recent
878 shifts in the distribution of marine species. *Polar Biology* **42**, 407–421. doi:10.1007/s00300-018-
879 2431-1.

880 Thorson, J.T. (2019a) Forecast skill for predicting distribution shifts: A retrospective experiment for
881 marine fishes in the Eastern Bering Sea. *Fish and Fisheries* **20**, 159–173. doi:10.1111/faf.12330.

882 Thorson, J.T. (2019b) Guidance for decisions using the Vector Autoregressive Spatio-Temporal (VAST)
883 package in stock, ecosystem, habitat and climate assessments. *Fisheries Research* **210**, 143–161.
884 doi:10.1016/j.fishres.2018.10.013.

885 Thorson, J.T. (2019) Measuring the impact of oceanographic indices on species distribution shifts: The
886 spatially varying effect of cold-pool extent in the eastern Bering Sea. *Limnology and*
887 *Oceanography* **0**. doi:10.1002/lno.11238.

888 Thorson, J.T. (2018) Three problems with the conventional delta-model for biomass sampling data, and a
889 computationally efficient alternative. *Canadian Journal of Fisheries and Aquatic Sciences* **75**,
890 1369–1382. doi:10.1139/cjfas-2017-0266.

891 Thorson, J.T. and Barnett, L.A.K. (2017) Comparing estimates of abundance trends and distribution shifts
892 using single- and multispecies models of fishes and biogenic habitat. *ICES Journal of Marine*
893 *Science* **74**, 1311–1321. doi:10.1093/icesjms/fsw193.

894 Thorson, J.T., Ianelli, J.N., Larsen, E.A., Ries, L., Scheuerell, M.D., Szuwalski, C. and Zipkin, E.F. (2016)
895 Joint dynamic species distribution models: a tool for community ordination and spatio-temporal
896 monitoring. *Global Ecology and Biogeography* **25**, 1144–1158. doi:10.1111/geb.12464.
897 Thorson, J.T. and Kristensen, K. (2016) Implementing a generic method for bias correction in statistical
898 models using random effects, with spatial and population dynamics examples. *Fisheries*
899 *Research* **175**, 66–74. doi:10.1016/j.fishres.2015.11.016.
900 Thorson, J.T., Munch, S.B. and Swain, D.P. (2017) Estimating partial regulation in spatiotemporal models
901 of community dynamics. *Ecology* **98**, 1277–1289. doi:10.1002/ecy.1760.
902 Tittensor, D.P., Eddy, T.D., Lotze, H.K., et al. (2018) A protocol for the intercomparison of marine fishery
903 and ecosystem models: Fish-MIP v1.0. *Geoscientific Model Development* **11**, 1421–1442.
904 doi:10.5194/gmd-11-1421-2018.
905 Tommasi, D., Stock, C.A., Hobday, A.J., et al. (2017) Managing living marine resources in a dynamic
906 environment: The role of seasonal to decadal climate forecasts. *Progress in Oceanography* **152**,
907 15–49. doi:10.1016/j.pocean.2016.12.011.
908 Van Kirk, K.F., Quinn, T.J. and Collie, J.S. (2010) A multispecies age-structured assessment model for the
909 Gulf of Alaska. *Canadian Journal of Fisheries and Aquatic Sciences* **67**, 1135–1148.
910 doi:10.1139/F10-053.
911 Von Szalay, P.G. and Raring, N.W. (2016) Data report: 2015 Gulf of Alaska bottom trawl survey. NMFS-
912 AFSC-325. US Department of Commerce, National Oceanic and Atmospheric Administration,
913 National Marine Fisheries Service, Alaska Fisheries Science Center, Seattle, WA.
914 Walters, C.J., Christensen, V., Martell, S.J. and Kitchell, J.F. (2005) Possible ecosystem impacts of
915 applying MSY policies from single-species assessment. *ICES Journal of Marine Science* **62**, 558–
916 568. doi:10.1016/j.icesjms.2004.12.005.
917 Walther, Y.M. and Möllmann, C. (2014) Bringing integrated ecosystem assessments to real life: a
918 scientific framework for ICES. *ICES Journal of Marine Science* **71**, 1183–1186.
919 doi:10.1093/icesjms/fst161.
920 Wetzell, C.R., Cronin-Fine, L. and Johnson, K.F. (2017) Status of Pacific ocean perch (*Sebastes alutus*)
921 along the US west coast in 2017. Northwest Fisheries Science Center, National Marine Fisheries
922 Service, Seattle, WA.
923
924

925 Table 1 – Model selection among candidate models, showing the model name (see Section 2.3 in
 926 main text for details), the marginal log-likelihood of the maximum likelihood estimate, the
 927 number of fixed effects, and the Akaike Information Criterion score for each model (where the
 928 most parsimonious model has $\Delta AIC = 0$ and models with $\Delta AIC < 3$ have some statistical
 929 support (Burnham and Anderson 2002))

Model	Negative log-likelihood	Number of parameters	ΔAIC
Index standardization	142867.2	160	6.6
Complete density dependence	143019.9	56	103.9
Same density dependence	142971.6	57	9.3
Different density dependence	142964.4	60	1
Species interactions	142959.9	64	0

930

931 Table 2 – Estimated interactions from the “species interactions” model (listing standard errors in
 932 parentheses), specifically listing **B – I** such that the element in the “arrowtooth” column and
 933 “Alaska pollock” row shows that a 1% increase in density for arrowtooth is estimated to cause a
 934 -0.07 decrease in per-capita productivity for Alaska pollock.

		Impact of a 1% increase in density of ...			
		Arrowtooth	Alaska pollock	Pacific cod	Pacific halibut
... on per-capita productivity of ...	Arrowtooth	-0.28 (0.06)	-0.05 (0.02)	-0.04 (0.03)	0.12 (0.06)
	Alaska pollock	-0.07 (0.06)	-0.32 (0.04)	0.03 (0.02)	-0.10 (0.07)
	Pacific cod	0.07 (0.04)	-0.05 (0.02)	-0.40 (0.04)	0.10 (0.06)
	Pacific halibut	0.06 (0.04)	-0.04 (0.02)	-0.03 (0.02)	-0.28 (0.07)

935

936

937 Fig. 1 – Total biomass for each species in each of five models (see legend in top-left panel for
938 color codes and Appendix B for detailed model descriptions), as well as fishing mortality rate
939 (black dashed line with scale on right-hand y-axis) for each species. Note that the “index
940 standardization” (black dashed lines) and “complete density dependence” (grey solid lines)
941 models predict biomass only in years with available data and are shown as lines with whiskers
942 (+/- one standard error), while other models predict biomass in years without sampling and are
943 shown as a shaded interval (+/- one standard error)

944

945 Fig. 2 – Biological reference points estimated by three MICE-in-space models (i.e., excluding
946 the “index-standardization” and “complete density dependence” models which cannot estimate
947 biological reference points), where b_{targ} is 40% of estimated biomass in the absence of fishing,
948 and f_{targ} is the fishing mortality estimated to result in biomass equal to b_{targ} on average.

949

950 Fig. 3 – Estimates of the natural logarithm of biomass density from the AIC-selected “species
951 interactions” model (red: high density; blue: low density) for each species (columns) in several
952 years (rows), where the first year (top row) shows the estimate of unfished biomass. Years are
953 chosen for illustration to be approximately even spaced but only using years with available
954 survey data, and where the density legend is identical among species and years and has units
955 $\ln(kg \cdot km^{-2})$

956

957 Fig. 4 – Estimated stock status (y-axis) for each year (x-axis), measured using a fishing intensity
958 ratio (left column: $f_{ratio}(c, t)$) and biomass ratio ($b_{ratio}(c, t)$, see Eq. 11) for each species
959 (rows) and the three MICE-in-space models that estimate biological reference points (see legend
960 in bottom-right panel for color codes). Each panel shows the maximum likelihood estimate
961 (central line) and ± 1 standard error (shaded area and outer lines), as well as the corresponding
962 target (horizontal dotted line); note that y-axes differ between panels.

963

964 Fig. 5 – Illustration of simulation experiment, showing natural logarithm of unfished biomass
965 density (1st and 2nd rows) and population density in 2015 (3rd and 4th rows) in units
966 $\ln(kg \cdot km^{-2})$ for the two species included in the estimation model (columns), where the
967 colorbar is shown in the bottom-right panel (red is high density and blue is low density). This
968 illustration allows comparison of true simulated density (1st and 3rd rows) vs. estimated density
969 (2nd and 4th rows) when simulating a new data set conditional on fixed effects estimated from
970 real-world data. Note that the simulation model simulates density for four species at a fine
971 spatial scale (using $n_x = 100$ knots), while the estimation model estimates density for only two
972 species at a coarse spatial scale (using $n_x = 50$ knots). For visual clarity, we do not show

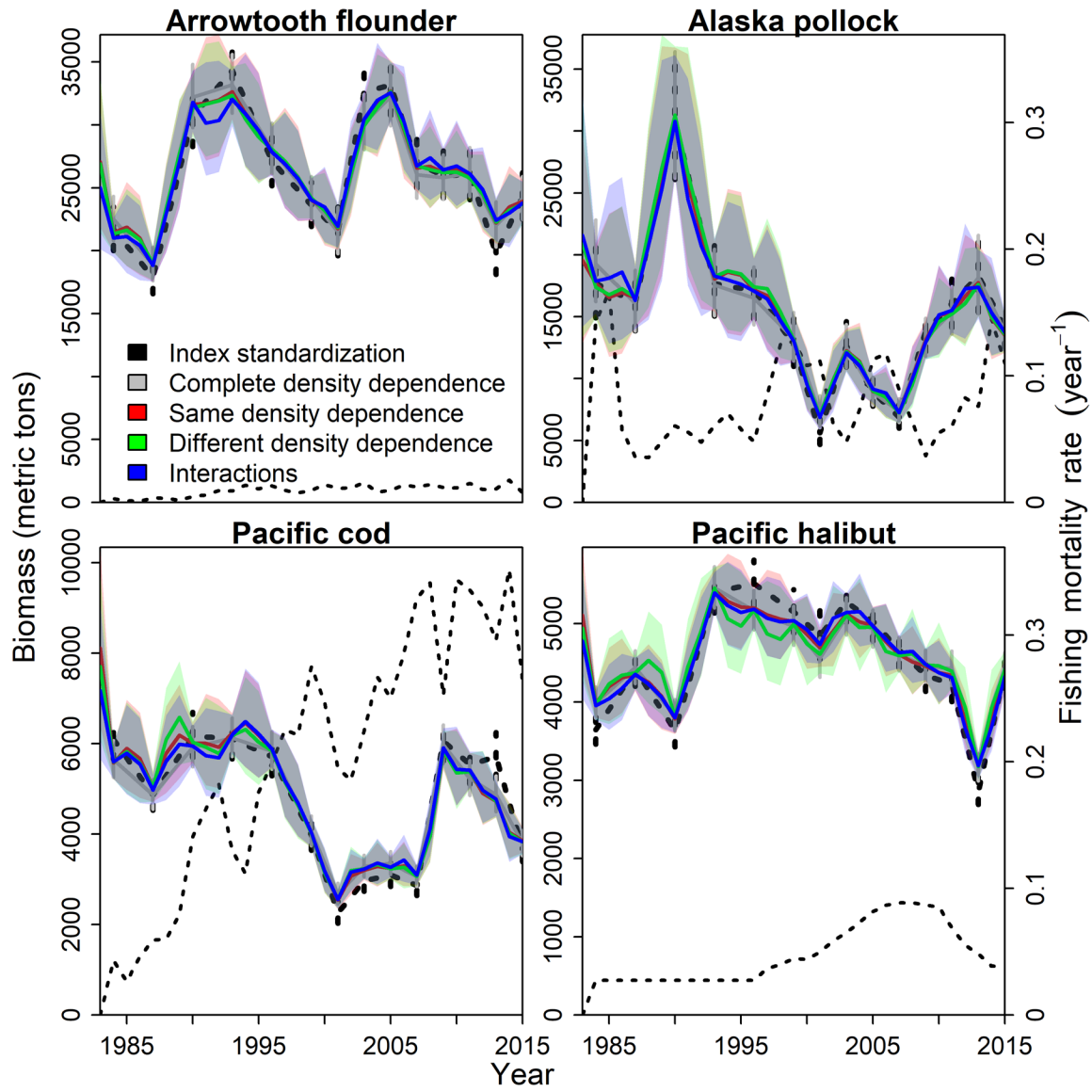
973 simulated density for the two species that are not then included in the estimation model for each
974 simulation replicate.

975

976 Fig. 6 – Illustration of results from a simulation experiment where each panel shows the
977 frequency distribution (y-axis) for different estimated values (x-axis), specifically showing
978 estimates of the interaction matrix \mathbf{B} (Fig. 6A) or biological reference points including fishing
979 mortality resulting in 40% of average unfished biomass, $\mathbf{f}_{0.4}$ (Fig. 6B left column) or the relative
980 error in estimates of unfished biomass, \mathbf{b}_{targ} (Fig. 6B, right column) from a simulation
981 experiment generating data based on the AIC-selected “species interactions” model, and then
982 restricting data to two species (arrowtooth and Alaska pollock) and fitting at a coarse spatial
983 resolution (50 knots). Each panel in the visualization of the interaction matrix (Fig. 6A) shows a
984 histogram of estimates from each simulation replicate, where the true value is indicated by a
985 vertical dashed line and the mean and standard deviation of estimates is listed (see Table 2 for
986 true values). The visualization of biological reference points (Fig. 6B) similarly shows a
987 histogram of estimates and the true value, and again lists the mean and standard deviation of
988 estimates.

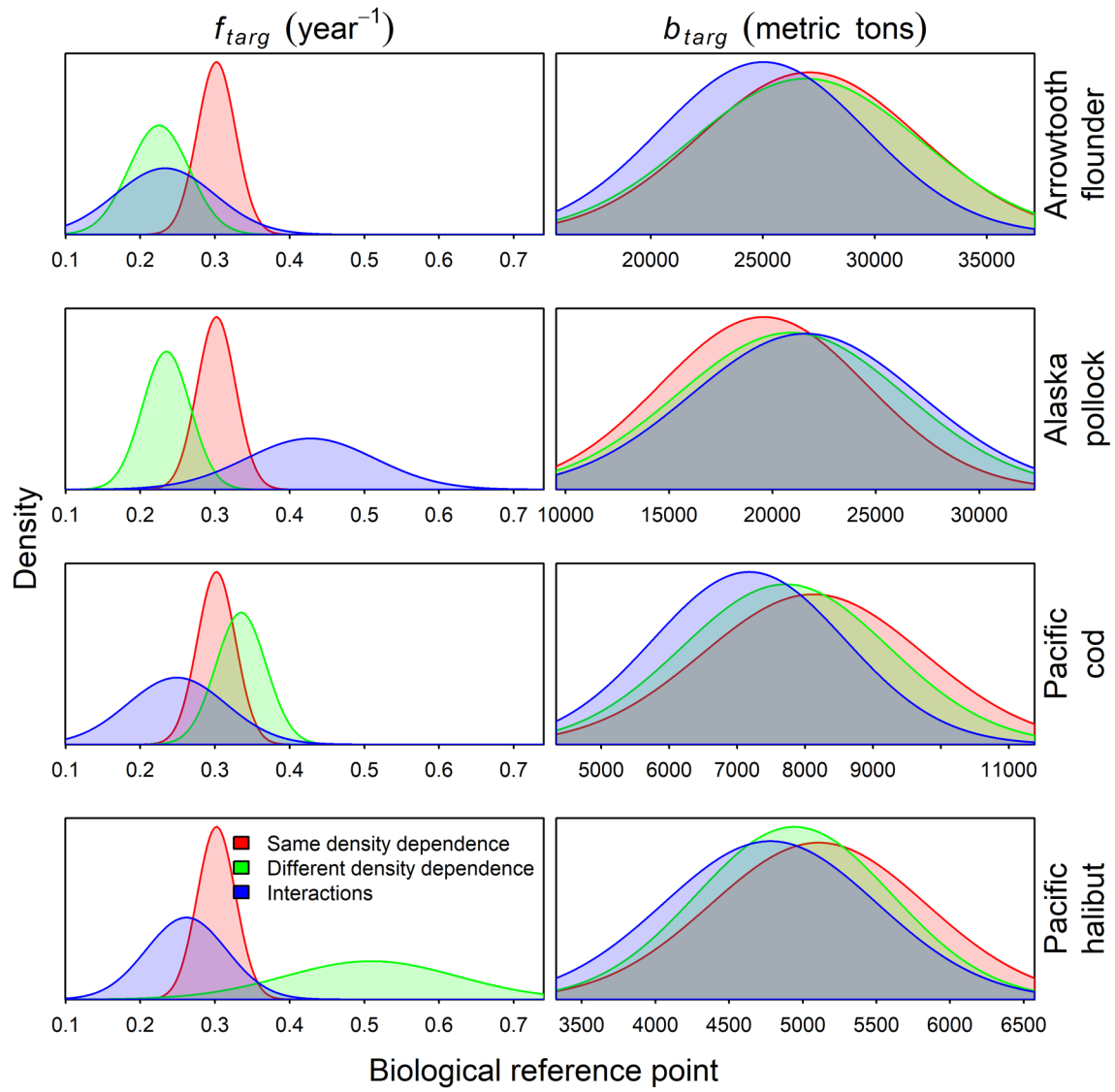
989

990 Fig. 1

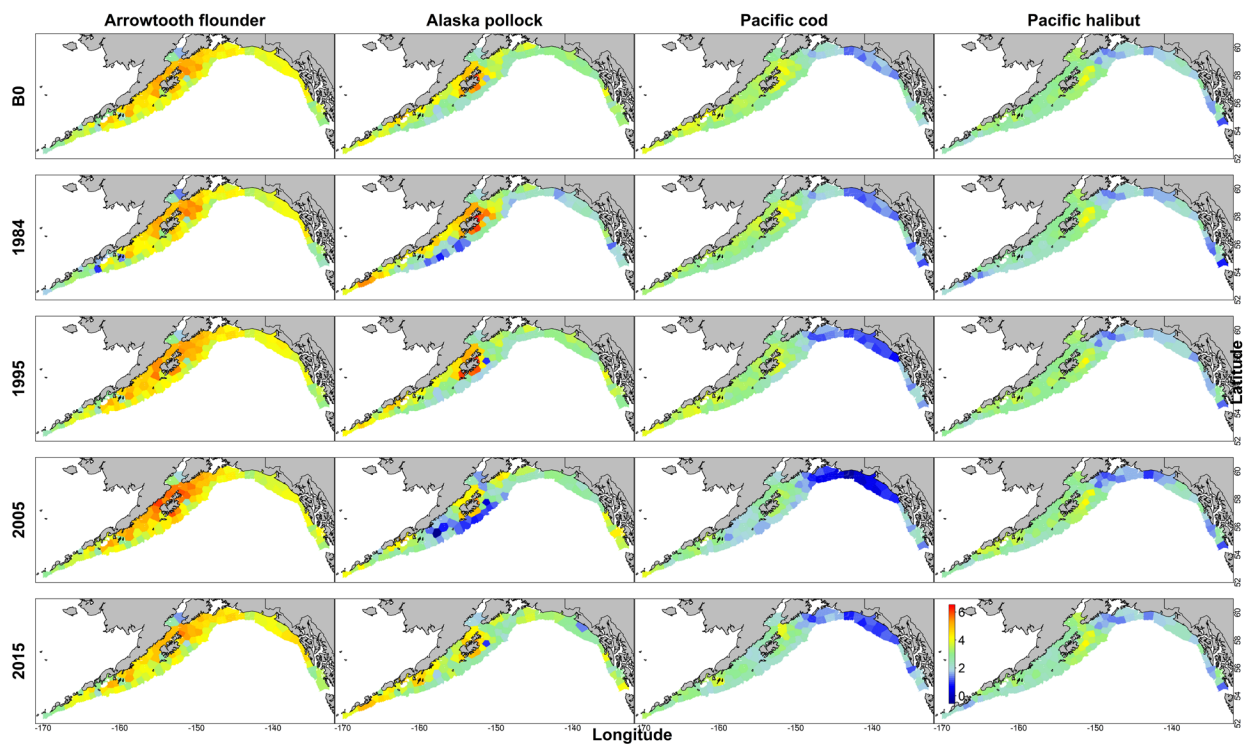


991

992

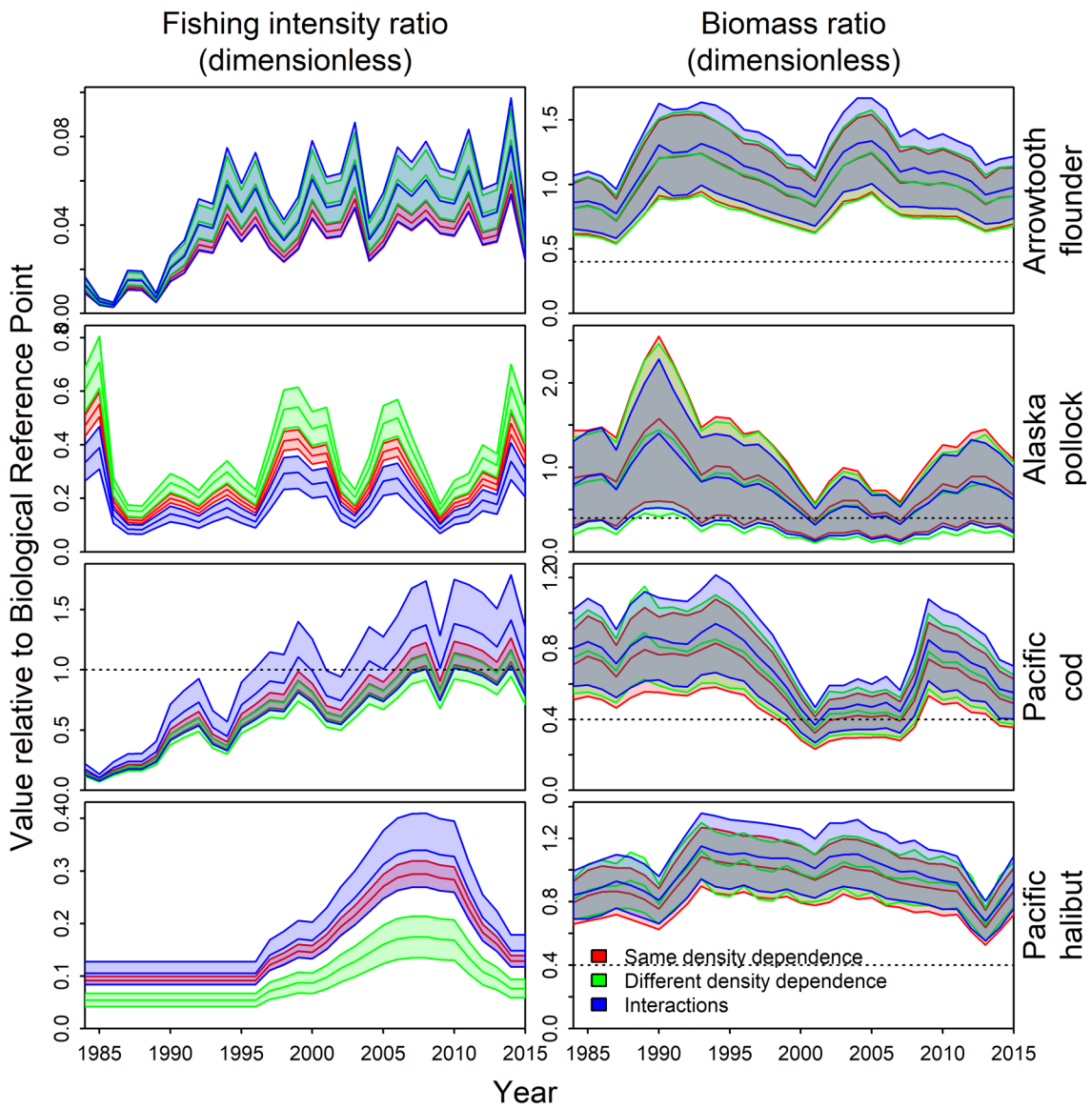


996 Fig. 3



997

998



1000

1001

